

EFFECTS OF GEOMETRIC NONLINEARITY ON STRESS ANALYSIS IN LARGE AMPLITUDE VIBRATION OF THIN CIRCULAR FUNCTIONALLY GRADED PLATES WITH RIGID CORE

F. Fotros, M.H. Pashaei* and R.A. Alashti

Department of Mechanical Engineering, Babol Noshirvani University of Technology
P.O. Box 484, Babol, Iran
farshad_f81@yahoo.com, mpashaei@nit.ac.ir, raalashti@nit.ac.ir

M.H. Naei

Department of Mechanical Engineering, University of Tehran
Tehran, Iran
mhnaei@ut.ac.ir

*Corresponding Author

(Received: February 19, 2011 – Accepted in Revised Form: September 18, 2011)

doi: 10.5829/idosi.ije.2011.24.03a.07

Abstract In this paper, the nonlinear free and forced axisymmetric vibration of a thin circular plate made of functionally graded material (FGM) with rigid core has been studied. This plate is formulated in terms of von-Karman's dynamic equation. In this study a semi-analytical approach is developed. For harmonic vibrations, by using assumed-time-mode method and Kantorovich time averaging technique, the governing equations are solved. This problem is solved using MATLAB code. FGM properties vary through the thickness of the plate. FGMs are spatial composites in which material properties vary continuously as well as non-homogeneity. The mass of the core respect to the mass of plate is negligible. For verification, a coreless FGM circular plate has been solved using this code. The results show a good approximation. The results reveal that the vibration amplitude and volume fraction have significant effects on the resultant stresses in large amplitude vibration of the functionally graded plate with rigid core.

Keywords Stress, Vibration, FGM, Circular plate, Rigid Core

چکیده در این مقاله ارتعاش آزاد و اجباری غیر خطی یک صفحه ساخته شده از ماده FGM بررسی شده است. این صفحه دایروی با تقارن محوری دارای یک هسته صلب در وسطش می باشد. معادلات حاکم بر این صفحه با استفاده از معادلات دینامیکی ون-کارمن به دست آمده است. برای انجام این مطالعه یک روش نیمه تحلیلی مورد استفاده قرار گرفته است. برای حل معادلات حاکم بر این ارتعاش هارمونیک از تکنیک متوسط زمانی کانتروویچ و assumed-time-mode و نیز از کد نوشته شده در Matlab استفاده شده است. مواد FGM مواد مرکب بخصوصی هستند که خواص آنها بطور پیوسته و نامتجانس تغییر می کند. خواص ماده FGM در این مطالعه در طول ضخامت آن تغییر می کند. جرم هسته در مقایسه با جرم صفحه ناچیز می باشد. برای اعتبارسنجی نتایج به دست آمده یک صفحه FGM بدون هسته با کد نوشته شده در این مطالعه حل شده است. نتایج این حل سازگاری خوبی را با نتایج موجود نشان می دهد که دلیل بر درستی کارکرد کد مورد استفاده می باشد. نتایج این تحقیق نشان می دهد که دامنه ارتعاش و کسر حجمی تاثیر قابل توجهی بر تنش بوجود آمده دارند.

1. INTRODUCTION

Consider a thin circular plate with uniform

thickness h and rigid core, Material of the plate is FGM. The present paper considers the vibration of a circular plate with a finite, axisymmetric, rigid

core attached. This case is an annular with a clamped interior edge. However, for rigid core without mass, the boundary conditions at the connection rigid core to the plate have been considered. Thin circular and annular plates are used in many engineering applications. They are often subjected to severe dynamic loading conditions, and can exhibit large amplitude vibrations of the order of the plate thickness. In this case, a significant geometrical nonlinearity is induced. Hence, the linear model would not be sufficient to predict the behavior of the plate. Therefore, the dynamic analog of the von-Karman equations, as the nonlinear equations of motion for thin plates have been used widely, especially for space vehicles and automobiles.

Functionally graded materials (FGMs) are inhomogeneous composite materials and are made from different phases of materials such as ceramics and metals. FGMs have different applications in defense industries, electronics, and biomedical sectors. Properties of FGMs vary continuously from one interface to the other. This is achieved by gradually varying volume fraction of constituent materials.

Reddy and Cheng [2] studied the harmonic vibration problem of functionally graded plates by means of a three-dimensional asymptotic theory formulated in terms of transfer matrix.

Allahverdizadeh and Naei [3] studied Nonlinear free and forced vibration analysis of thin circular functionally graded plates and investigated the amplitude and thermal effects on the nonlinear behavior of those plates. They also studied the effects of large vibration amplitudes on the stresses of thin circular functionally graded plates.

Chen [4] analyzed the nonlinear vibration of a shear deformable functionally graded plate by using the equations that include the effects of transverse shear deformable and rotary inertia.

Amini, et al [5] studied stress analysis for thick annular functionally graded plate. They used first-order shear deformation plate and von Kármán-type equation.

Their results revealed that vibration amplitude and volume fraction have significant effect on resultant stresses in large amplitude vibration of functionally graded thick plate.

The aim of the present paper is to study nonlinear free vibration of thin circular

functionally graded plates with rigid core. Material properties are assumed to be graded in the thickness direction according to a simple power law distribution in terms of the volume fractions of the constituents.

The formulations are based on Classic Plate Theory and von Kármán-type equation. For harmonic vibration by using assumed-time-mode method sinusoidal oscillations are assumed, then the time variable is eliminated by applying Kantorovich averaging method. Therefore, the basic governing equations for the problem are reduced to a pair of ordinary differential equations which form a nonlinear boundary value problem.

Shooting method is used to the numerical study of these governing equations.

Extensive numerical results are presented in both dimensionless tabular and graphical forms, and highlight the influence of material composition and ratio of rigid core radiuses on induced stresses in large amplitude vibration of thin circular functionally graded plates with rigid core.

2. THEORETICAL DEVELOPMENT

In this paper mass of the rigid core is considered negligible. Also, the radius of the rigid core is not constant. This is fraction of the plate radius. Consequently, some terms which are dependent upon the weight of the rigid core have been eliminated.

For thin plate, there are several theories; from that von-Karman's large deflection theory which provides a good approximation and is usually applied has been used in this study.

2.1. Properties of Functionally Graded Material

FGMs are typically made of a combination of ceramic and metal or a combination of different metals. In the present study the FGMs composed of metal and ceramic have been considered. The Thickness of the plate is constant and equal to h . The top surface ($z=h/2$) of the plate is ceramic-rich whereas the bottom surface ($z=-h/2$) is metal-rich. Material properties P of the functionally graded plate are assumed to vary through the thickness of the plate, as a function of the volume fraction and properties of the constituent materials. These

properties can be expressed as

$$P = \sum_{i=1}^n P_i V_i, P = E, \rho, \alpha, K, \nu \quad (1)$$

where P_i and V_i are the material properties and volume fraction of the constituent material i . It is clear that the sum of volume fractions of the constituent materials, should be

$$\sum_{i=1}^n V_i = 1 \quad (2)$$

To start with, a simple law definition for the volume fraction across the thickness of the plate is assumed. This is defined as:

$$V_i = \left(\frac{2z+h}{2h}\right)^n \quad (3)$$

Volume fraction index n dictates the material variation profile across the plate thickness. This simple rule of mixture model does provide a reasonably accurate prediction of the mechanical as well as thermal properties of these inhomogeneous materials.

From Equations 1 to 4, one has:

$$P(z) = (P_c - P_m) \left(\frac{2z+h}{2h}\right)^n + P_m \quad (4)$$

in which indices (c) and (m) indicate ceramic and metal, respectively. In what follows, the FGM is combined of stainless steel (SUS304) and silicon nitride (Si3N4). Detail of this FGM is presented in

Table 1.

2.2. Governing Equations Consider a thin circular FGM plate with rigid core subjected to axisymmetric transverse load and cylindrical coordinates r , θ , and z , located in its initially undeformed configuration.

The direction of the r -coordinate is radially outward from the center, the z -coordinate along the thickness, and the

θ -coordinate is directed along a circumference of the plate (Figure 1).

The thickness of the FGM plate is h , the radius of the plate $r=a$ and rigid core radius is $r=c$.

The radial displacement u_r and the transverse displacement u_z show the displacement of the point with (r,z) coordinate. By using the Kirchhoff plate theory, the radial displacement u_r and the transverse displacement u_z are expressed as,

$$u_r(r, z, t) = u(r, t) - zw(r, t),_r \quad (5)$$

$$u_z(r, z, t) = w(r, t) \quad (6)$$

where $u(r, t)$ and $w(r, t)$ are the radial and transverse displacements of the point on the middle surface of the plate respectively, and t is the time variable.

On the basis of geometric non-linear theory of thin plates in von Karman's sense, one obtains the strain-displacement relations:

$$\varepsilon_r = \frac{\partial u}{\partial r} + \frac{1}{2} \left(\frac{\partial w}{\partial r}\right)^2 - z \frac{\partial^2 w}{\partial r^2} \quad (7)$$

TABLE 1. Temperature- Dependent Coefficients of Material Properties [3].

Property	Material	P ₋₁	P ₀	P ₁	P ₂	P ₃
E(GPa)	Si ₃ N ₄	0	384.43e9	-3.070e-4	2.160e-7	-8.946e-11
	SUS304	0	201.04e9	3.079e-4	-6.534e-7	0
ρ (kg/m ³)	Si ₃ N ₄	0	2,370	0	0	0
	SUS304	0	8,166	0	0	0
	Si ₃ N ₄	-	0.2400			
	SUS304		0.3177	-	-	-

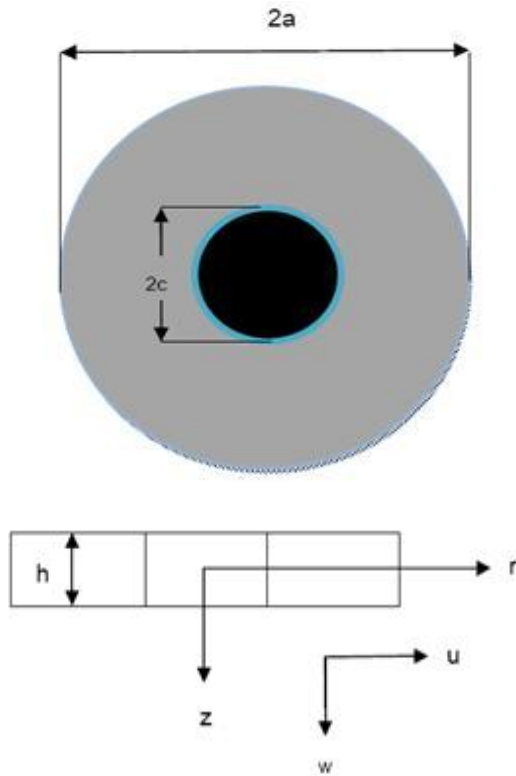


Figure 1. Geometry and co-ordinates of the plate

$$\varepsilon_{\theta} = \frac{u}{r} - \frac{z}{r} \frac{\partial w}{\partial r} \quad (8)$$

where ε_r and ε_{θ} are the radial and tangential strains, respectively. The constitutive equations are given as follows:

$$s_r = \frac{E(z,T)}{1-\nu} \left[\frac{1}{1+\nu} (e_r + \nu e_{\theta}) \right] \quad (9)$$

$$s_{\theta} = \frac{E(z,T)}{1-\nu} \left[\frac{1}{1+\nu} (e_{\theta} + \nu e_r) \right] \quad (10)$$

$$E(z,T) = E_{cm}(T) \left(\frac{2z+h}{2h} \right)^n + E_m(T) \quad (11)$$

$$E_{cm} = E_c - E_m \quad (12)$$

The membrane forces, and the bending moments are defined as:

$$(N_r, N_{\theta}) = \int_{-\frac{h}{2}}^{\frac{h}{2}} (s_r, s_{\theta}) dz \quad (13)$$

$$(M_r, M_{\theta}) = \int_{-\frac{h}{2}}^{\frac{h}{2}} (s_r, s_{\theta}) z dz \quad (14)$$

N_r, N_{θ} the membrane forces, and M_r, M_{θ} the bending moments, where σ_r and σ_{θ} are the stresses, $E(z,T)$ the elastic module, and ν the Poisson ratios.

Now by substituting Equations 9 and 10 into Equations 13 and 14 and integrating, the resultant moments and forces can be calculated.

Governing equations for nonlinear vibration of the plates in cylindrical coordinate can be expressed as follows.

$$(rN_r)_{,r} - N_{\theta} = 0 \quad (15)$$

$$(rQ_r)_{,r} + (rN_r w_{,r})_{,r} + rP(r,t) = h.I.r.w_{,tt}$$

$$I = \left(\frac{r_{cm}}{n+1} + r_m \right), r_{cm} = r_c - r_m \quad (16)$$

$$(rM_r)_{,r} - M_{\theta} - rQ_r = 0 \quad (17)$$

$P(r,t)$ is the uniformly distributed lateral intensity, Q_r is the shearing force per unit length.

By eliminating the radial displacement function $u(r,t)$ from the results of Equations 13 the compatibility equation is obtained with the aid of Equation 15:

$$(N_r + N_{\theta})_{,r} = \frac{-hA}{2r} (w_{,r})^2 \quad (18)$$

when the stress function $\psi(r,\theta)$, and the corresponding relations

$$N_r = \frac{\Psi}{r}, N_{\theta} = \Psi_{,r} \quad (19)$$

Combining Equations (18) and (19) gives:

$$\Psi_{,rr} + \frac{1}{r} \Psi_{,r} - \frac{\Psi}{r^2} = \frac{-hA}{2r} (w_{,r})^2 \quad (20)$$

Combining results of Equation 14 and 19, and moment equilibrium about a circumferential tangent, one may obtain:

$$-\left(\frac{h^3(B)^2}{(A)(1-\nu^2)} - \frac{h^3(R)}{1-\nu^2} \right) (\nabla^4 w) - \left(\frac{1}{r} (y w_{,r})_{,r} + h \left(\frac{r_{cm}}{n+1} + r_m \right) w_{,tt} \right)$$

$$-\frac{h^2(B)}{1-\nu^2} \left[\frac{r}{h(A)} (\Psi_{,rrr}) + \frac{5-\nu}{h(A)} (\Psi_{,rr}) + \frac{3-2\nu}{rh(A)} (\Psi_{,r}) + \frac{\nu}{r^2 h(A)} (\Psi) - \frac{\nu}{r^3 h(A)} (\Psi) \right]$$

$$-\frac{h^2(B)}{1-\nu^2} \left[(w_{,r})(w_{,rrr}) + (w_{,rr})^2 + \frac{2-\nu}{r} (w_{,r})(w_{,rr}) \right] = P(r,t) \quad (21)$$

where

$$\nabla^4 w = w_{,rrrr} + \frac{2}{r} w_{,rrr} - \frac{1}{r^2} w_{,rr} + \frac{1}{r^3} w_{,r} \quad (22)$$

Since the principal vibration takes place in direction perpendicular to the middle plane, it is reasonable to neglect the longitudinal and rotary inertias.

Equations 20 and 21 are dynamic forms of von-Karman's equations, where the longitudinal and rotary inertias are neglected.

By introducing dimensionless variables as

$$r^* = r/a, \quad h^* = h/a, \quad c^* = c/a, \quad u^* = u/a, \quad w^* = w/a,$$

$$\phi = \psi/(aE_m), \quad t = 1/a\sqrt{E_m/r_m}t, \quad \Omega^* = a\sqrt{r_m/E_m}\Omega,$$

$$q(r^*, t) = P(r, t)/E_m \quad (23)$$

where Ω is the linear natural frequency.

By using the dimensionless variables, the governing equations can now be written in nondimensional form. In the following equations and relations we eliminate the (*) for simplicity.

$$f_{,rr} + \frac{1}{r} f_{,r} - \frac{f}{r^2} = \frac{-hA}{2r} (w_{,r})^2 \quad (24)$$

$$-\left(\frac{h^3(B)}{(A)(1-\nu^2)} - \frac{h^3(R)}{1-\nu^2} \right) (\nabla^4 w) - \frac{1}{r} (fw_{,r})_{,r} + h \left(\frac{rcm}{n+1} + 1 \right) w_{,tt}$$

$$-\frac{h^2(B)}{1-\nu^2} \left[\frac{r}{h(A)} (f_{,rrrr}) + \frac{5-\nu}{h(A)} (f_{,rrr}) + \frac{3-2\nu}{rh(A)} (f_{,rr}) \right.$$

$$\left. + \frac{\nu}{r^2 h(A)} (f_{,r}) - \frac{\nu}{r^3 h(A)} (f) \right]$$

$$-\frac{h^2(B)}{1-\nu^2} \left[(w_{,r})(w_{,rrr}) + (w_{,rr})^2 + \frac{2-\nu}{r} (w_{,r})(w_{,rr}) \right] = q(r,t) \quad (25)$$

3. BOUNDARY CONDITIONS

In order to solve governing Equations 24 and 25, they must be accompanied by a set of boundary conditions at both inner and outer boundary for any time t . The boundary conditions are

Inner radius:

$$w_{,r}(c,t) = 0, \quad u(c,t) = 0 \quad (26)$$

Outer radius:

$$w(a,t) = 0, \quad w_{,r}(a,t) = 0, \quad u(a,t) = 0 \quad (27)$$

An exact solution of the differential Equations 24 and 25 which satisfy boundary conditions of the form (26) and (27) is at present unknown.

The coefficients A, B, R are given in Appendix. In the analysis and solution, the method of "assumed-time-mode" has been used. Assuming an appropriate harmonic response for non-linear vibrations, the time variable is eliminated by using a Kantorovich averaging method [1], and a non-linear boundary value problem is obtained including spatial variables. This boundary value problem is solved numerically.

4. APPROXIMATE ANALYSIS

Despite many researches on the nonlinear behavior of plates, there is still no analytical solution for Equations 24 and 25. The reason lies in coupling nature of governing equations as well as the non-linear terms of the derivatives of displacements.

The standard Fourier analysis used in linear vibration problems cannot be applied in an exact sense due to nonlinear character of differential equations which causes a coupling of vibration modes.

In the analysis and solution of this kind of equations two approximate methods are commonly used. One is known as "assumed-space-mode" solution, which is generally achieved by taking some assumed spatial shape function and by using a variation method to eliminate the spatial variables and reduce the partial differential equations to ordinary ones only including time as independent variable [6,7].

Another method is “assumed-time-mode” solution. In this method, a simple harmonic function in time is assumed and is then eliminated from the equation of motion using the Kantorovich averaging procedure [8-10].

The resulting nonlinear boundary value problem is solved numerically. In the present investigation, the latter method is employed.

4.1. Kantorovich averaging method Firstly, it is assumed that the plate is imposed by a harmonic load of the following form

$$q(r, t) = Q(r) \sin \Omega t \quad (28)$$

For the purpose of the approximate analysis, the steady-state response is assumed to be as follows:

$$w(r, t) = G(r) \sin \Omega t \quad (29)$$

$$f(r, t) = F(r)(\sin \Omega t)^2 \quad (30)$$

where $F(r)$ and $G(r)$ are undetermined shape functions of vibration. The assumption $\emptyset(r, \tau)$ follows from Equation 30 and for $F(r)$ is consistent with the fact that the radial displacement of any point of the plate is independent of the up or down position of the plate.

By substituting Equations 29 and 30 into the governing Equation 13, one finds,

$$F_{,rr} + \frac{1}{r} F_{,r} - \frac{F}{r^2} = -\frac{h(A)}{2r} (G_{,r})^2 \quad (31)$$

Expressions (28-30) cannot satisfy Equation 14 for all values of τ . equating the average virtual work over one period oscillation zero yields:

$$\begin{aligned} & -\left(\frac{h^3(B)^2}{(A)(1-\nu^2)} - \frac{h^3(R)}{1-\nu^2}\right)(\nabla^4 G) - \frac{3}{4} \frac{1}{r} (FG_{,r})_{,r} \\ & - h\left(\frac{r_{cm}}{n+1} + 1\right)\Omega^2 G - \frac{h^2(B)}{1-\nu^2} (G_{,rr}) = Q(r) \end{aligned} \quad (32)$$

Set of Equations 31 and 32 along with boundary conditions (26) and (27) compose the two-point nonlinear boundary value problem which governs the large amplitude vibration of a thin circular FGM plate with rigid core.

Now, the non-dimensional boundary conditions of the thin circular FGM plate with rigid core:

$$\begin{cases} r=c: \\ G_{,r}=0 \\ G_{,rr} = -\left(\frac{1-n^2}{ah^3(R)}\right)\left(\frac{Q(r)c}{2}\right) - \frac{a}{c}(G_{,rr}) \\ F(r)_{,r} \frac{na}{c} F(r) \end{cases} \quad (33)$$

where c is non-dimensional rigid core's radius. The circular plate edge is clamped at $r=1$, so the boundary conditions can be expressed as:

$$\begin{cases} r=1: \\ G=0 \\ G_{,r}=0 \\ F(r)_{,r} - u F(r)=0 \end{cases} \quad (34)$$

4.2. First-Order Differential Equations By introducing new variables as:

$$\begin{aligned} Z(r) &= [G, G_{,r}, G_{,rr}, G_{,rrr}, F, F_{,r}]^T \\ &= [z_1, z_2, z_3, z_4, z_5, z_6]^T \end{aligned} \quad (35)$$

$$\begin{bmatrix} G_{,r} \\ G_{,rr} \\ G_{,rrr} \\ G_{,rrrr} \\ F_{,r} \\ F_{,rr} \end{bmatrix} = \begin{bmatrix} z_2 \\ z_3 \\ z_4 \\ z_{4,r} \\ z_6 \\ z_{6,r} \end{bmatrix} = \begin{bmatrix} z_{1,r} \\ z_{2,r} \\ z_{3,r} \\ z_{4,r} \\ z_{5,r} \\ z_{6,r} \end{bmatrix} = \begin{bmatrix} f_1 \\ f_2 \\ f_3 \\ f_4 \\ f_5 \\ f_6 \end{bmatrix} \quad (36)$$

First, the higher order equations must be rewritten as a first order differential equation form like

$$z_{1,r} = z_2 \quad (37)$$

$$\begin{aligned} z_{2,r} &= z_3 \\ z_{3,r} &= z_4 \end{aligned} \quad (38)$$

$$\begin{aligned} z_{4,r} &= -\frac{2}{r} z_4 + \frac{1}{r^2} z_3 - \frac{1}{r^3} z_2 \\ & - \left(\frac{1}{\left(\frac{h^3 B^2}{A(1-\nu^2)} - \frac{h^3 R}{1-\nu^2}\right)}\right) \left[\frac{3}{4r} (z_2 z_6 + z_3 z_5)\right] \end{aligned} \quad (39)$$

$$+ h\left(\frac{r_{cm}}{n+1} + 1\right)I z_1 + \left(\frac{h^3 B}{1-\nu^2}\right) z_3 + Q] \quad (40)$$

$$z_{5,r} = z_6 \quad (41)$$

$$z_{6,r} = -\frac{1}{r} z_6 + \frac{1}{r^2} z_5 - \left(\frac{hA}{2r}\right) z_2^2 \quad (42)$$

where $\lambda=\Omega^2$ and the boundary conditions are:

$$r=c: \begin{cases} z_2 = 0 \\ z_4 = -\left(\frac{1-\nu^2}{h^3 R}\right)\left(\frac{Qc}{2}\right) - \frac{1}{c} z_3 \\ z_6 = \frac{\nu}{c} z_5 \end{cases} \quad (43)$$

$$r=1: \begin{cases} z_1 = 0 \\ z_2 = 0 \\ z_6 = uz_5 \end{cases} \quad (44)$$

5. VERIFICATION OF RESULTS

In order to show the reliability of the numerical technique employed in this study, some numerical tests have been carried out. In order to validate the results of the present study the linear and nonlinear steady-state free and forced vibration of a clamped circular FGM plate without rigid core has been solved using this method. In this case a coreless plate with thickness ratio of $h/r_o=0.1$, volume fraction index $n=10$ has been investigated and the results have been compared with those of Ref. [3].

Figure 2 shows the harmonic response of the clamped circular coreless FGM plate in transverse vibration. In this figure the close agreement between the results of this study and the results of Ref. [3] can be observed.

This figure describes the influence of amplitude on the non-dimensional linear and nonlinear frequencies (ω_b) of FGM plate in free ($Q=0$) and forced ($Q=1.5 \cdot 10^{-9}$) vibration around the first mode.

6. NUMERICAL RESULTS AND DISCUSSIONS

The first nonlinear normalized axisymmetric mode shapes for various values of n are plotted in Figure 3. Effect of various values of n on the mode shape is negligible.

The diagram of Figure 4 has been drawn from the contact place of plate with the rigid core at the radius of 0.1. The stress on the contact place at r^*

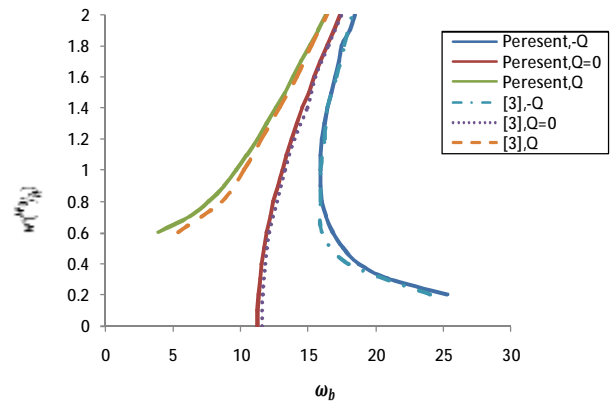


Figure 2. Harmonic response of the clamped circular coreless FGM plate around the first mode for the uniformly distributed load ($Q=1.5 \cdot 10^{-9}$), values taken from Ref. [3], read from graph.

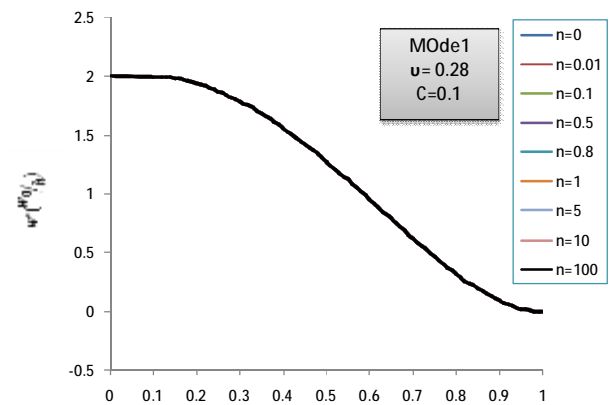


Figure 3. Nonlinear normalized axisymmetric mode shapes of the clamped circular FG plate with rigid core for different values of n at the First Mode.

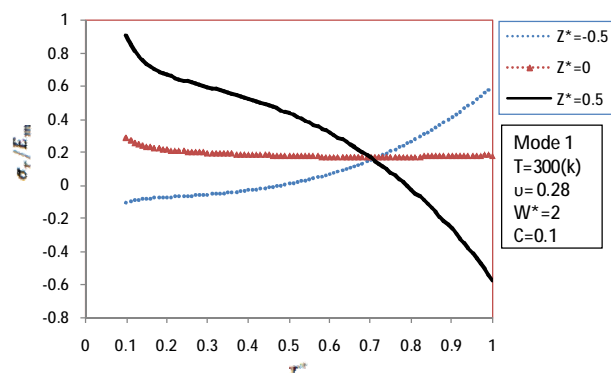


Figure 4. Variation of dimensionless radial stress with dimensionless radius on metal-rich and neutral and rich-ceramic surface for rigid core radius 0.1.

=0.1 is more than those of other places around as it may be seen in the figure. This relative increase of the stress is due to the clamped contact of the core to the plate. Such conditions are present at the outer edge of core at $r^*=1$. In other words, the amount of the stress at the outer edge is more than those of other neighboring places.

The radius of the rigid core from $r^*=0.1$ in Figure 4 has been increased to $r^*=0.2$ in Figure 5. So, the diagram in Figure 5 has been drawn for $r^*=0.2$.

As it is shown in the figures, the stress at the geometrical middle surface ($z^*=0$) remains unchanged.

The dimensionless radial stresses of a circular FGM with different rigid core radius has been obtained. A comparison of these stresses is shown in Figure 6. This diagram is drawn for pure metal. From this figure it may be seen that with the increasing of the radius of the core the radial stresses increase.

Comparison of the circumferential stresses is shown in Figure 7.

The stresses with minus sign are of compressive and those with plus sign are tensile. There is no common sense on the change of circumferential stress.

In Figures 8(a,b) and 9, it is obvious that increasing n , will decrease the amount of the stresses. For metal rich plates ($n \approx 0$), the stress distribution is linear, where for the FGM plate; the behavior is nonlinear and is governed by the variation of the properties in the thickness direction.

The material properties of functionally graded plate are assumed to vary through the thickness of the plate; therefore, mid plane of the plate is different from the neutral surface. Since the Young's modulus of the ceramic is greater than that of the metal, the neutral plane is closer to the ceramic-rich surface.

Figures 10 and 11 show variation of the dimensionless radial and circumferential stresses versus the dimensionless radius on metal-rich surface.

As may be seen from the figures by increasing the n and reducing $E(z)$ the amount of the dimensionless stresses has been reduced. Also, the figures show that the stress at the centre of the core is negative, while at the outer radius is positive.

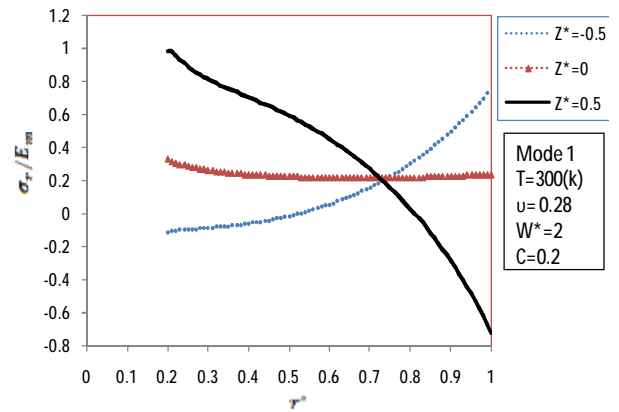


Figure 5. Variation of dimensionless radial stress with dimensionless radius on metal-rich & neutral & rich-ceramic surface for rigid core radius 0.2.

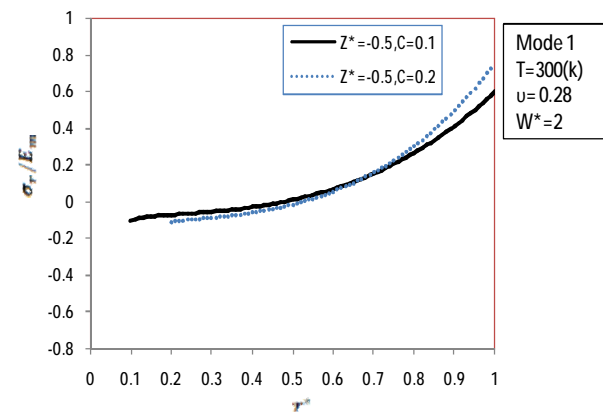


Figure 6. Comparison between dimensionless radial stress on metal-rich surface for rigid core radii 0.1 and 0.2 .

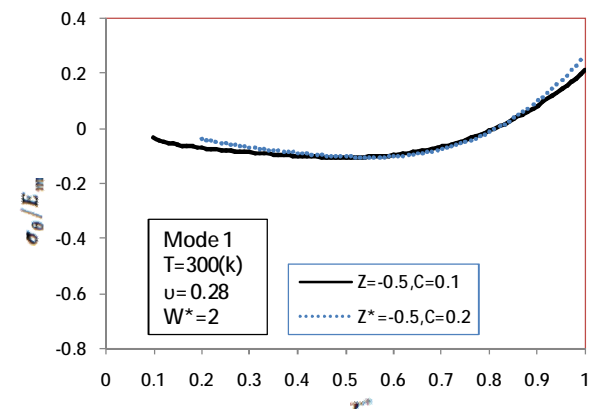
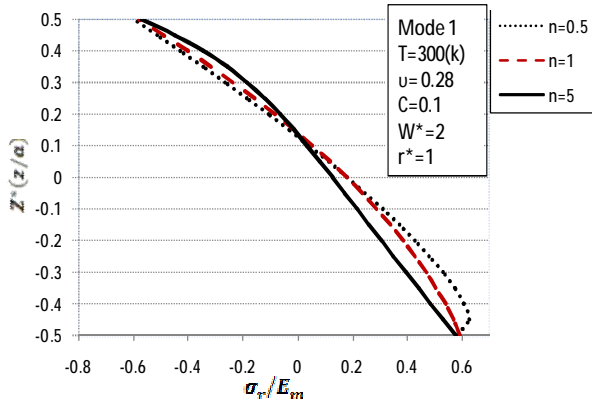
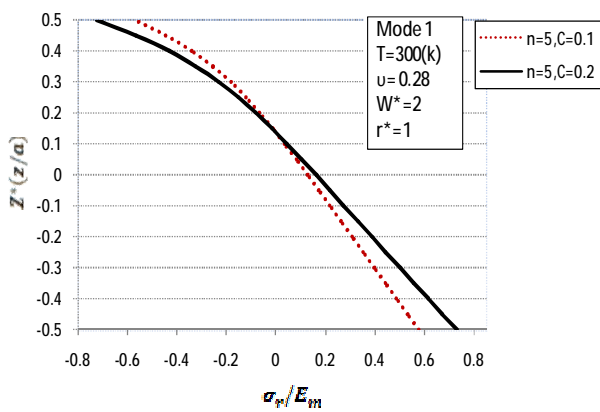


Figure 7. Comparison between dimensionless circumferential stress on metal-rich surface for rigid core radii 0.1 and 0.2.



(a)



(b)

Figure 8. (a) Variation of the dimensionless radial stress along the thickness of the plate at outer radius for plate with rigid core radius $C=0.1$ and (b) Comparison between dimensionless radial stress along the thickness for different rigid core radii $C=0.1$ and $C=0.2$.

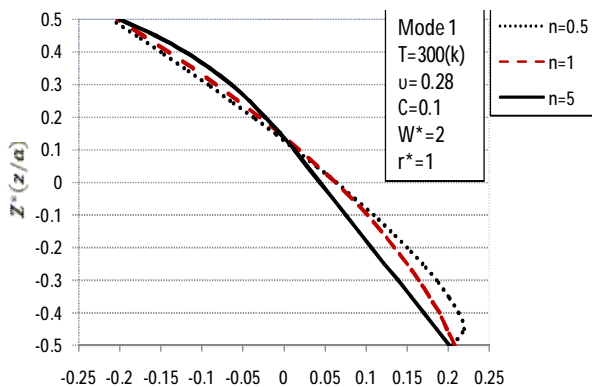


Figure 9. Variation of the dimensionless circumferential stress along the thickness of the plate at outer radius for plate with rigid core radius $C=0.1$.

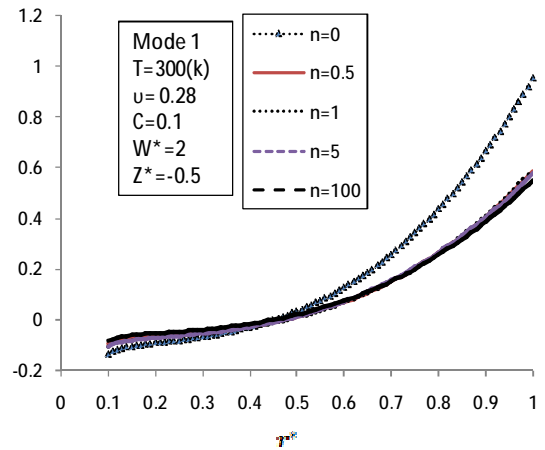


Figure 10. Variation of the dimensionless radial stress with the dimensionless radius on metal-rich surface.

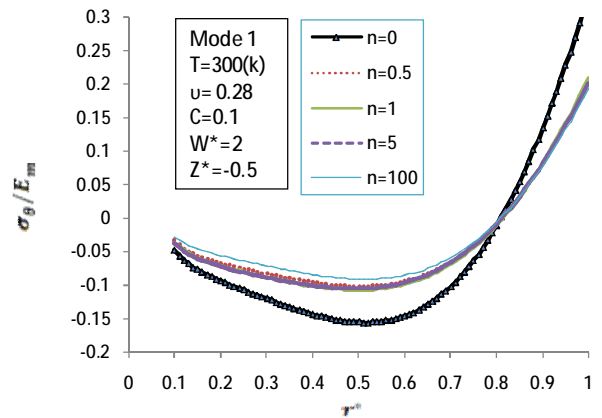


Figure 11. Variation of the dimensionless circumferential stress with the dimensionless radius on metal-rich surface.

7. CONCLUSION

Large amplitude vibration of a thin circular functionally graded plate with rigid core has been investigated in this paper by using Classic-plate theory and von-Karman -type equation. The effect of volume fraction index and change of the radius of rigid core has been studied. For the low vibration amplitudes, different amounts of volume fraction index as well as radius of the rigid core affect the stress, while different values of volume fraction index have considerable effect on the stresses in high vibration amplitudes.

The FGM properties vary through the constant thickness of the plate. Reduction of volume fraction index causes the dimensionless modulus of elasticity to be reduced. Consequently, the dimensionless stress has been reduced.

In the ceramic-rich surface as well as the metal-rich surface, the stress is distributed linearly on the transverse section, whereas, the FGM plate with rigid core experiences a nonlinear stress distribution. Also, the middle plane of the rigid plate differs from its neutral plane; by increasing the dimensionless radius of the core, the radial stress rises. However, an exact decision may not be made on the circumferential stress.

8. APPENDIX

Definition of variables A, B, D, R, and S

$$B = \frac{nE_{cm}}{2(n+1)(n+2)} \quad (\text{A.1})$$

$$A = \left(E_m + \frac{E_{cm}}{n+1}\right) \quad (\text{A.2})$$

$$R = \frac{E_m}{12} + \frac{(n^2 + n + 2)}{4(n+1)(n+2)(n+3)} E_{cm} \quad (\text{A.3})$$

9. REFERENCES

1. Li, S.-R., Zhou, Y.-H. and Song, X., "Nonlinear vibration and thermal buckling of an orthotropic annular plate with a centric rigid mass", *J. Sound Vibration*, Vol. 251, (2002), 141–152.
2. Reddy, J.N., Cheng, Z.Q., "Frequency of functionally graded plates with three-dimensional asymptotic approach", *J. Eng. Mech.*, Vol. 129, (2003), 896–900.
3. Allahverdizadeh, A., Naei, M.H. and Nikkhah Bahrami, M., "Nonlinear free and forced vibration analysis of thin circular functionally graded plates", *Journal of Sound and Vibration*, Vol. 310, (2007), 966–984.
4. Chen, C.-S., "Nonlinear vibration of a shear deformable functionally graded plate", *J. Compos. Struct.*, Vol. 68, (2005), 295–302.
5. Amini, H., Rastgoo, A. and Soleimani, M., "Stress analysis for thick annular FGM plate", *J. of Solid Mechanics*, Vol. 4, (2009), 328-342.
6. Huang X.L., Shen, H.S., "Nonlinear vibration and dynamic response of functionally graded plates in thermal environments", *International Journal of Solids and Structures*, Vol. 41, (2004), 2403-2427.
7. Huang S., "Non-linear vibration of a hinged orthotropic circular plate with a concentric rigid mass", *Journal of Sound and Vibration*, Vol. 214, 91998), 873-883.
8. Huang, C.L., Aurora, P.R., "Non-linear oscillations of elastic orthotropic annular plates of variable thickness", *Journal of Sound and Vibration*, Vol. 62, (1979), 443-453.
9. Huang C.L.D. and Wolker, H.S., "Non-linear vibration of hinged circular plate with a concentric rigid mass", *Journal of Sound and Vibration*, Vol. 126, (1988), 9-17.
10. Li, S.R., "Non-linear vibration and thermal buckling of a heated annular plate with a central rigid mass", *Applied Mathematics and Mechanics* (English edition) Vol. 13, (1992), 771-777.